

RESEARCH ARTICLE OPEN ACCESS

Design of a Solar-Wind Hybrid Renewable Energy System for Power Quality Enhancement: A Case Study of 2.5 MW Real Time Domestic Grid

F. Max Savio¹ | S. Vinson Joshua² | K. Usha³ | Muhammad Faheem^{4,5} | Raju Kannadasan⁶ | Arfat Ahmad Khan⁷

¹Department of Electrical and Electronics Engineering, Saveetha Engineering College, Chennai, India | ²Department of Electronics and Communication Engineering, Vel Tech Rangarajan Dr. Sagunthala R & D Institute of Science and Technology, Chennai, India | ³Department of Electrical and Electronics Engineering, Sri Sivasubramaniya Nadar (SSN) College of Engineering, Chennai, India | ⁴School of Technology and Innovations, University of Vaasa, Vaasa, Finland | ⁵VTT-Technical Research Centre of Finland Ltd., Espoo, Finland | ⁶Department of Electrical and Electronics Engineering, Sri Venkateswara College of Engineering, Sriperumbudur, India | ⁷Department of Computer Science, College of Computing, Khon Kaen University, Khon Kaen, Thailand

Correspondence: Muhammad Faheem (muhammf@uwasa.fi)

Received: 11 September 2024 | **Revised:** 10 November 2024 | **Accepted:** 8 December 2024

Keywords: grid interface | harmonic distortions | hybrid renewable energy | smart grid | solar PV | wind energy

ABSTRACT

The increasing global energy demand driven by climate change, technological advancements, and population growth necessitates the development of sustainable solutions. This research investigates the design, modeling, and simulation of a 2.5 MW solar-wind hybrid renewable energy system (SWH-RES) optimized for domestic grid applications. A survey conducted across 450 households identified a total energy demand of 2.3 MW, with distinct day and night usage profiles. In response, a hybrid system consisting of a 1.5 MW solar park and a 1 MW wind energy unit was designed to ensure continuous power supply. The system was modeled and simulated using MATLAB, and its performance was evaluated through a detailed Total Harmonic Distortion (THD) analysis. This research addresses the critical need for a sustainable and high-quality power supply by designing, modeling, and simulating a 2.5 MW solar-wind hybrid renewable energy system (SWH-RES) optimized to meet the energy demand of a surveyed 2.3 MW domestic load, while also reducing THD to acceptable levels for improved power quality and grid stability. The results demonstrated a significant reduction in THD, with voltage THD decreasing from 45.48% to 26.20% and current THD from 8.32% to 2.88% after implementing filtering components. These findings underscore the effectiveness of the proposed SWH-RES in providing stable, high-quality power while addressing the growing demand for sustainable energy solutions.

1 | Introduction

Global energy demand has been on a consistent rise, driven by factors such as population growth, industrialization, and technological advancements. This trend has led to increased reliance on fossil fuels, which are not only finite but also contribute significantly to environmental degradation and climate change. As a result, there is a pressing need to transition towards sustainable and renewable energy sources that can meet the growing energy

demands without further harming the environment. Among the various renewable energy sources, solar and wind energy have emerged as leading alternatives due to their abundance, sustainability, and relatively low environmental impact [1, 2].

Solar and wind energy systems, when combined as hybrid systems, offer several advantages over single-source renewable energy systems. The complementary nature of solar and wind resources—where solar energy is most available during daylight

This is an open access article under the terms of the [Creative Commons Attribution](https://creativecommons.org/licenses/by/4.0/) License, which permits use, distribution and reproduction in any medium, provided the original work is properly cited.

© 2025 The Author(s). *Engineering Reports* published by John Wiley & Sons Ltd.

hours and wind energy can be harnessed at different times of the day—makes hybrid systems more reliable and efficient. These systems can significantly reduce the intermittency issues associated with renewable energy sources, providing a more consistent and stable power supply [2, 3]. The integration of a solar-wind hybrid renewable energy system (SWH-RES) into domestic grid applications, therefore, represents a promising solution for reducing dependence on fossil fuels and lowering greenhouse gas emissions [4, 5]. However, the implementation of SWH-RES in domestic grid systems is not without challenges. One of the primary technical challenges is the generation of harmonics, which are distortions in the electrical waveform that can affect the stability and efficiency of the power system. Harmonics are often caused by nonlinear loads and can lead to several problems, including increased losses, overheating of equipment, and reduced system efficiency [3]. Minimizing total harmonic distortion (THD) is, therefore, essential for the successful deployment of SWH-RES in domestic grid applications [5].

This study focuses on the design, modeling, and simulation of a 2.5 MW SWH-RES specifically tailored for domestic grid applications. The system design is informed by an energy consumption survey conducted across 450 households, which revealed a peak energy demand of 2.3 MW. To meet this demand, the proposed SWH-RES integrates a 1.5 MW solar park and a 1 MW wind energy unit. These units are synchronized to provide a continuous and reliable power supply. Additionally, the system incorporates capacitor banks for energy storage, which are crucial for maintaining a stable power output, particularly during periods of low energy generation from either source. A critical aspect of the proposed system is the optimization of the interfacing unit and the control strategy used in the three-phase inverter, which is designed to minimize THD. The system's performance is evaluated through mathematical modeling and simulation using MATLAB. The results are compared with analytical data, focusing on THD values to ensure that the proposed system can provide a reliable and sustainable power supply for domestic grids without compromising on power quality [4].

In the nutshell, this study contributes to the ongoing efforts to transition from non-renewable to renewable energy sources by demonstrating the feasibility of a SWH-RES for domestic grid applications. The successful reduction of THD in the proposed system underscores its potential for widespread adoption, offering a sustainable solution to meet the growing energy demands of households while mitigating environmental impacts.

2 | Literature Review

The integration of renewable energy sources into domestic and utility-scale grid systems has been a subject of extensive research over the past few decades. The literature on solar, wind, and hybrid renewable energy systems highlights the growing interest in reducing reliance on fossil fuels and addressing the challenges associated with renewable energy generation. This section provides a review of key studies focusing on the design, optimization, and harmonics analysis of solar-wind hybrid renewable energy systems (SWH-RES), emphasizing their relevance to the present study.

Solar energy systems, particularly photovoltaic (PV) systems, have become increasingly prevalent due to their capacity to convert sunlight directly into electricity with minimal environmental impact. This adoption is driven by the need for sustainable energy solutions and advancements in PV technology. Numerous studies have explored various aspects of PV systems, including their design, efficiency, and integration into the grid. The efficiency of PV systems is a critical factor influencing their performance and adoption. Fadi Al-Turjman et al. [6] highlight that the efficiency of PV systems is significantly affected by several parameters, including irradiance levels, temperature, and the orientation of solar panels. Variations in solar irradiance can lead to fluctuating energy outputs, making it essential to optimize the placement and angle of PV panels to maximize their exposure to sunlight. Temperature also plays a crucial role, as high temperatures can reduce the efficiency of PV cells by increasing their resistance. Consequently, effective thermal management strategies are necessary to maintain optimal operating conditions and enhance energy conversion efficiency.

In addition to efficiency, the economic feasibility of PV systems is a major consideration for their widespread adoption. Roy et al. [7] examines the cost-effectiveness of solar energy systems for domestic applications, emphasizing the importance of reducing installation and maintenance costs to make solar technology more accessible to homeowners. The initial investment for PV systems can be substantial, but advancements in technology and economies of scale have led to a decrease in costs over time. Government incentives, such as tax credits and rebates, also play a significant role in improving the economic viability of solar energy [7, 8]. Moreover, integrating PV systems into the grid presents both opportunities and challenges. The intermittent nature of solar energy requires careful management to ensure a stable and reliable power supply. Researchers like Hamid et al. [9] have investigated grid integration strategies, such as the use of energy storage systems and advanced grid management techniques, to address the variability of solar power. Energy storage solutions, such as batteries and pumped hydro storage, can help mitigate the impact of fluctuations in solar energy generation by storing excess power for use during periods of low sunlight [9, 10].

In addition to grid integration, the environmental benefits of PV systems are significant. Unlike fossil fuels, solar energy generation does not produce greenhouse gases or other pollutants, making it a cleaner alternative for reducing the carbon footprint of energy consumption [11]. Furthermore, the lifecycle analysis of PV systems demonstrates that the environmental impact associated with their manufacturing, operation, and disposal is relatively low compared to conventional energy sources [12]. Overall, the widespread adoption of solar energy systems is supported by advances in technology, reductions in costs, and the growing recognition of their environmental benefits. As research continues to address the challenges of efficiency, economic feasibility, and grid integration, PV systems are expected to play a central role in the transition to a more sustainable energy future.

Wind energy systems, particularly those utilizing wind turbines, play a pivotal role in the renewable energy landscape by converting the kinetic energy of wind into electricity. These systems offer a complementary solution to solar energy, particularly in regions

where wind patterns are favorable and consistent. Research by Mustafa Kamal et al. and Murugesan et al. [13, 14] emphasizes the effectiveness of wind energy systems in harnessing wind resources to provide a reliable power supply, especially in areas where solar energy may be less consistent due to geographical or climatic factors. Wind turbines, which are central to wind energy systems, operate by converting wind flow into mechanical energy through the rotation of blades. This mechanical energy is then converted into electrical energy by a generator. According to a study by Tabbi Wilberforce et al. [15], the efficiency of wind turbines is influenced by factors such as wind speed, turbine design, and the height of the turbine. High wind speeds and optimized turbine designs can significantly enhance energy generation, making wind turbines a viable option for renewable energy production.

Despite their benefits, wind energy systems face challenges, particularly due to the intermittent nature of wind. Unlike solar energy, which can be harnessed during daylight hours, wind energy can vary significantly depending on local wind conditions. This variability poses a challenge for grid integration and energy reliability. Studies by Muhammad Khalid et al. [16] have shown that the integration of wind energy into the grid requires advanced forecasting and energy management strategies to address fluctuations in wind power output. To mitigate the intermittency of wind energy, researchers have explored hybrid renewable energy systems that combine wind and solar power. Such hybrid systems leverage the complementary nature of wind and solar resources to provide a more stable and continuous power supply. For example, Alphonse Ngila Mulumba et al. [17] found that integrating wind and solar energy sources can reduce the overall variability of power generation and enhance the reliability of energy supply. By combining these two sources, hybrid systems can balance periods of low wind with periods of high solar generation, and vice versa.

The development of hybrid systems also involves the use of energy storage solutions to manage power fluctuations. Energy storage technologies, such as batteries and pumped hydro storage, can store excess energy generated during periods of high wind or solar output and release it during periods of low generation [18]. This approach helps smooth out the variability and provides a more reliable power supply to the grid. Furthermore, the environmental impact of wind energy systems is generally favorable compared to fossil fuel-based energy sources. Wind turbines produce no greenhouse gas emissions during operation, making them a clean alternative for reducing carbon footprints [19]. However, the environmental impact of turbine manufacturing and land use should also be considered. A lifecycle analysis by Atilgan Turkmen et al. [20] highlights that while wind energy systems have low operational emissions, their manufacturing and installation phases can have localized environmental effects.

Hybrid renewable energy systems (HRES), particularly those that combine solar and wind energy, have gained significant attention for their ability to address the intermittency challenges associated with single-source renewable systems. These hybrid systems leverage the complementary nature of solar and wind resources to provide a more stable and reliable power supply. By integrating both types of energy sources, HRES can produce electricity

during times when one resource is unavailable, thus ensuring a continuous power supply. The primary advantage of combining solar and wind energy is the mitigation of the intermittency issue that affects each resource individually. Solar energy is available during daylight hours and is influenced by weather conditions and seasonal variations, while wind energy depends on wind speed and can vary throughout the day and year. By integrating these two sources, hybrid systems can provide a more consistent energy output, as periods of low wind can be offset by high solar generation and vice versa. This complementary nature enhances the overall reliability of power supply compared to single-source systems [21].

Research by Tianhong Pan et al. [22] has explored the design and optimization of solar-wind hybrid renewable energy systems (SWH-RES) for domestic grid applications. Their study emphasizes the critical role of system sizing and the integration of energy storage solutions to maximize the benefits of hybrid systems. Proper sizing ensures that the system can meet the specific energy demands of a household or facility, reducing reliance on non-renewable backup power. The inclusion of energy storage, such as batteries or pumped hydro storage, allows excess energy generated during peak production times to be stored and used during periods of low generation, further stabilizing the power supply [16]. Moreover, the economic feasibility of SWH-RES is a key consideration for widespread adoption. The initial investment for installing both solar panels and wind turbines, along with energy storage systems, can be substantial. However, studies have shown that the long-term benefits, including reduced energy bills and lower carbon emissions, can outweigh the initial costs [10]. Additionally, advancements in technology and reductions in component costs have made hybrid systems more affordable and accessible [8].

Hybrid systems also contribute to grid stability and reliability by providing a diversified energy supply. According to Mansoor Urf Manoo et al. [23], integrating multiple renewable sources helps to balance the variability of individual resources and enhances grid resilience. This approach is particularly beneficial for remote or off-grid areas where traditional energy infrastructure may be limited or non-existent. Overall, hybrid renewable energy systems that combine solar and wind resources offer a promising solution to the challenges of intermittency and reliability associated with single-source renewable systems [24]. By optimizing system design, integrating energy storage, and considering economic factors, SWH-RES can provide a stable and sustainable power supply for various applications. Ongoing research and technological advancements will continue to enhance the efficiency and feasibility of these systems, supporting their broader adoption and contribution to a sustainable energy future [25, 26].

One of the critical challenges in integrating renewable energy systems into the grid is the generation of harmonics, which can distort the electrical waveform and compromise system efficiency. Harmonics, which are typically caused by nonlinear loads such as inverters, can lead to various issues including increased losses, overheating of electrical components, and reduced overall power quality [27]. Harmonics are unwanted frequencies that are integer multiples of the fundamental frequency (50 or 60 Hz) of the electrical system. They arise due to the non-linear characteristics

of devices such as rectifiers, inverters, and other power electronics used in renewable energy systems. According to a study by Zhe Hu et al. [28], these harmonics can cause significant problems in power systems, including voltage distortion, which can affect the operation of sensitive equipment and lead to inefficiencies in power transmission. In renewable energy systems, particularly hybrid systems combining solar and wind energy, the use of inverters is crucial for converting the generated direct current (DC) into alternating current (AC) that is compatible with the grid. However, the switching processes within inverters can introduce harmonics into the electrical system [29]. The impact of these harmonics can be substantial, leading to issues such as increased heating in transformers and cables, potential damage to electrical equipment, and overall degradation of power quality.

Reguieg et al. [30] have extensively studied the impact of harmonics in renewable energy systems, particularly in hybrid systems that combine solar and wind energy. Their research highlights the importance of addressing harmonics to ensure the smooth operation of the grid. The study emphasizes the need for advanced inverter control techniques to minimize total harmonic distortion (THD), which is a measure of the extent of harmonic distortion present in the system. To mitigate the impact of harmonics, several strategies can be employed. One approach is the use of passive or active filters, which are designed to filter out specific harmonic frequencies and improve power quality. Passive filters, which use components such as inductors, capacitors, and resistors, are commonly used but can be less effective in dynamically varying conditions [31]. Active filters, on the other hand, use power electronic devices to adaptively cancel out harmonics and are more versatile [32]. Another effective strategy is the application of advanced control algorithms in inverters. According to a study by Wang Guo et al. [33], techniques such as pulse-width modulation (PWM) and adaptive filtering can significantly reduce THD and improve the overall efficiency of renewable energy systems. These techniques involve adjusting the switching patterns of inverters to minimize harmonic generation and ensure cleaner power output. Additionally, proper system design and component selection play a crucial role in reducing harmonics. Careful design of the electrical network and selection of high-quality components can help minimize harmonic distortion and improve overall system performance [24]. Thamatapu et al. [34], have addressed the challenges of maintaining power reliability and stability in distribution systems, particularly in grid-connected hybrid renewable energy systems comprising photovoltaic (PV) and wind energy. A novel Distributed Power Flow Controller (DPFC) using Lion Optimization Algorithm (LOA) was designed to regulate power flow dynamically, adapting to fluctuations in renewable energy generation by adjusting the system's parameters, such as voltage and current, using signals derived from these parameters. According to Amar Ahmed et al. [35], when a hybrid system operates under non-ideal grid conditions, including voltage unbalance and distortions, it experiences multiple-order ripples in the machine, as well as in active and reactive power delivered to the grid. A Normalized Maximum Correntropy Criterion (NMCC)-based approach is designed to comprehensively suppress ripples caused by grid voltage unbalance and distortions across both positive and negative harmonic sequences, regardless of harmonic order. Also, Kanagaraj et al. [36], have addressed the challenges associated

with the fluctuating nature of renewable energy sources, specifically solar PV and wind. These energy sources depend heavily on current and predicted weather conditions, resulting in variable outputs that can disrupt electricity generation and grid stability. The issues were overcome by implementing a quasi-Z-Source Inverter (qZSI)-based STATCOM integrated into a three-phase, four-wire (3P4W) distribution network. This approach combines advanced inverter technology with intelligent control strategies, supporting the reliable integration of renewable energy sources into the grid [37–42].

The literature on solar, wind, and hybrid renewable energy systems underscores the potential of these technologies to address the growing energy demand while reducing environmental impact. The challenges associated with harmonics and the intermittency of renewable energy sources have driven research towards optimizing hybrid systems for grid integration. Also, the research gap from the literature work can be summarized to set as the objective of the proposed system:

- The numerous studies have explored the efficiency and grid integration of solar and wind energy systems but, the issue of harmonics generated by inverters remains a critical challenge that has not been fully addressed.
- Several studies on solar-wind hybrid renewable energy systems (SWH-RES), there remains a gap in the optimization of system sizing, configuration, and energy storage integration to maximize efficiency and economic feasibility.
- The intermittency of renewable energy sources poses a major challenge for grid stability, and while energy storage systems are proposed as a solution, their effectiveness and economic impact vary.

Addressing these research gaps will contribute to the development of more efficient, reliable, and economically viable hybrid renewable energy systems that are better suited for large-scale grid integration.

The insights gained from these studies are crucial for the development of efficient and reliable SWH-RES, as explored in this paper. By building on the existing body of knowledge, this study aims to further advance the understanding of hybrid renewable energy systems and their application in domestic grid settings.

3 | Case Study—Collection of Field Data

To address the power demand challenges and optimize the design of hybrid renewable energy systems, a detailed case study was conducted focusing on various houses in Tamil Nadu, India. The study aimed to collect and analyze real-time data on power consumption patterns to better understand the energy needs and to provide solutions for effective power management. Data was gathered from a diverse set of houses across different districts of Tamil Nadu. The survey is done for almost 420 houses in the community by 45 teams each visiting maximum of 10 houses (approximately) in the community. For the confidentiality of the real time data, the survey data of one house from each team is shown as a sample in the Table 1. This comprehensive data collection was crucial for accurately assessing

TABLE 1 | Survey details field data.

| Survey area | : | Sriperumbudur | | | | | | | | | | |
|------------------------------------|--------------------------------|------------------------------------|----|---|---|----|----|---|---|---|----|-------|
| No. of houses in the community | : | 600 (approx.) | | | | | | | | | | |
| No. of houses visited | : | 420 | | | | | | | | | | |
| No. of houses considered | : | 10 (randomly from different teams) | | | | | | | | | | |
| Power demand (for 10 houses) in kW | : | 89.17 KW | | | | | | | | | | |
| S. No | Houses | 1 | 2 | 3 | 4 | 5 | 6 | 7 | 8 | 9 | 10 | Count |
| 1 | LED light (5–20 W) | 8 | 35 | 9 | 8 | 10 | 10 | 5 | 6 | 9 | 20 | 120 |
| 2 | Celling fan (50–75 W) | 2 | 9 | 4 | 5 | 3 | 3 | 3 | 2 | 5 | 5 | 41 |
| 3 | Mixcy (400–750 W) | 0 | 2 | 0 | 1 | 0 | 0 | 1 | 0 | 1 | 2 | 7 |
| 4 | Grinder (500–1000 W) | 1 | 2 | 1 | 1 | 1 | 1 | 1 | 1 | 1 | 1 | 11 |
| 5 | Washing machines (1000–2000 W) | 1 | 2 | 1 | 1 | 1 | 1 | 1 | 0 | 0 | 1 | 9 |
| 6 | Iron box (1000–2000 W) | 1 | 2 | 1 | 1 | 0 | 1 | 1 | 1 | 1 | 2 | 11 |
| 7 | Laptops (50–100 W) | 1 | 2 | 0 | 1 | 0 | 1 | 0 | 1 | 1 | 1 | 8 |
| 8 | Pump motor (0.5–1 HP) | 1 | 1 | 1 | 1 | 1 | 1 | 1 | 1 | 2 | 1 | 11 |
| 9 | Air cooler (100–250 W) | 0 | 3 | 1 | 1 | 1 | 0 | 0 | 0 | 2 | 2 | 10 |
| 10 | Induction stove (1000–2000 W) | 0 | 0 | 0 | 0 | 1 | 0 | 0 | 0 | 1 | 1 | 3 |
| 11 | Refrigerator (100–400 W) | 1 | 2 | 1 | 1 | 2 | 1 | 1 | 1 | 1 | 2 | 13 |
| 12 | Heater (1000–2000 W) | 0 | 1 | 0 | 0 | 1 | 1 | 0 | 0 | 1 | 1 | 5 |
| 13 | TV (50–150 W) | 1 | 2 | 1 | 1 | 1 | 1 | 1 | 1 | 2 | 1 | 12 |
| 14 | Water purifier (25–60 W) | 1 | 2 | 1 | 1 | 1 | 1 | 1 | 1 | 1 | 1 | 11 |
| 15 | Tube lights (40–60 W) | 0 | 0 | 0 | 4 | 3 | 0 | 2 | 1 | 3 | 0 | 13 |
| 16 | Bed lamps (10–15 W) | 1 | 3 | 0 | 1 | 9 | 1 | 1 | 0 | 6 | 2 | 24 |
| 17 | Table fans (30–50 W) | 0 | 0 | 0 | 0 | 0 | 1 | 0 | 0 | 1 | 2 | 4 |
| 18 | Computers (200–600 W) | 1 | 0 | 0 | 0 | 0 | 0 | 0 | 0 | 1 | 1 | 3 |

the power demands and consumption patterns. The information collected included the power usage of various appliances, day and night-time energy consumption, and the average utilization hours of these appliances.

The data analysis revealed that the average utilization hours of appliances in the surveyed houses ranged from 60 to 100 h per week. This range indicates the variability in energy usage based on household size, lifestyle, and the types of appliances used. The power consumption values of these appliances were found to be between 3000 and 10,000 watts, depending on their type and usage frequency. For a more detailed analysis, day and night-time power consumption data was collected from approximately 10 houses. This detailed data allowed for a nuanced understanding of the energy requirements during different times of the day. Table 1 below summarizes the key details of the survey data:

The proposed system involves the energy harvesting from two renewable sources, solar PV and wind. It is necessary to calculate the power demand during the day time and night time to select the rating of the hybrid required to install.

The Table 2 provides a detailed breakdown of the power demand during the day and night. The information in the Tables 1 and 2 are shown in the Figure 1.

The total power demand for the community comprising 420 houses was calculated using a method similar to that detailed in Table 2. This comprehensive assessment involved aggregating the power consumption data from each household to estimate the overall energy requirements for both daytime and nighttime periods. The resulting figures, which represent the total power demand across the entire community, are summarized in Table 3. This table provides a consolidated view of the estimated power needs, offering valuable insights into the scale of energy requirements for effective planning and implementation of renewable energy systems. The power demand from 420 houses is graphically represented in the Figure 2.

4 | Modeling of SWH-RES

The modeling of the proposed Solar Wind Hybrid – Renewable Energy System (SWH-RES) is provided in this section. The nomenclature used in the modeling is given below.

| | |
|-------------------------|---|
| ρ | Air density (in kg/m^3), typically around 1.225 kg/m^3 at sea level under standard conditions |
| A | Swept area of the wind turbine blades (in m^2) |
| v | Wind velocity (m/s) |
| C_p | Power co-efficient |
| γ | Tip speed ratio |
| β | Pitch angle |
| R | Rotor radius (m) |
| ω | Frequency in (rad/s) |
| P_m | Aerodynamic wind turbine power (W) |
| T_m | Torque acting in the shaft (Nm) |
| i_{sd}, i_{sq} | Stator current in d and q axis, respectively. (A) |
| u_{sd}, u_{sq} | Stator voltage in d and q axis, respectively. (V) |
| L_{sd}, L_{sq} | Stator winding inductance in d and q axis, respectively. (H) |
| Ψ_p | Permanent flux (Wb) |
| ω_s | Speed of Stator flux (rad/s) |
| R_{sa} | Stator winding resistance (Ω) |
| T_e | Electromagnetic Torque (Nm) |
| I_{SC} | Short circuit current of the PV cell (A) |
| V_{OC} | Open circuit voltage of the PV cell (V) |
| V_{pv} | Photo-voltaic voltage (V) |
| I_{ph} | Photo-voltaic current (A) |
| k_i | Solar Current constant at 25°C |
| I_r | Solar irradiance (W/m^2) |
| T | Operating temperature (K) |
| I_0 | Saturation Current (A) |
| I_{rs} | Reverse saturation current (A) |
| q | Electron charge ($1.6 \times 10^{-19} \text{C}$) |
| R_{sh} | Shunt resistance (Ω) |
| N_s | Number of solar cells connected in series |
| N_p | Number of solar cells connected in parallel |
| k | Boltzmann's constant ($1.3805 \times 10^{-23} \text{ J/K}$) |
| E_{g0} | Band gap energy of the semiconductor (1.1 eV) |
| V_t | Diode thermal voltage (V) |
| N_{SBat} | Number of series batteries in battery bank |
| N_{PBat} | Number of parallel batteries in battery bank |
| V_{Bat} | Battery voltage (V) |
| SOC | State of charge |
| $\text{SOC}_i(t)$ | State of charge at the instance of time, t |
| I_{Bat} | Battery current (A) |
| Δt | Time change (sec) |
| $\eta_i(I_{kolBat(t)})$ | Battery efficiency |
| f_c | Cut-off frequency (Hz) |
| f_s | Switching frequency (Hz) |
| L_f | Filter inductance (H) |
| C_f | Filter capacitance (F) |
| I_{ac} | AC current (A) |
| V_{dc} | Dc-link voltage (V) |

TABLE 2 | Day time and night time power demand.

| Day time power demand | | | | |
|-----------------------|-----------|-------------|----------------------|--------------|
| House | Power (W) | Current (A) | Operating hours (Hr) | Amp. hr (Ah) |
| 1 | 3704 | 16.1 | 6 | 96.63 |
| 2 | 19,626 | 85.33 | 8 | 682.64 |
| 3 | 6761 | 29.4 | 5 | 146.98 |
| 4 | 7644 | 33.23 | 8 | 265.88 |
| 5 | 9603 | 41.75 | 7 | 292.27 |
| 6 | 5304 | 23.06 | 5 | 115.3 |
| 7 | 4289 | 18.65 | 5 | 93.24 |
| 8 | 2806 | 12.2 | 4 | 48.8 |
| 9 | 13,255 | 57.63 | 6 | 345.78 |
| 10 | 16,182 | 70.36 | 6 | 422.14 |
| Total | 89,174 | 388 | 60 | 2509.66 |

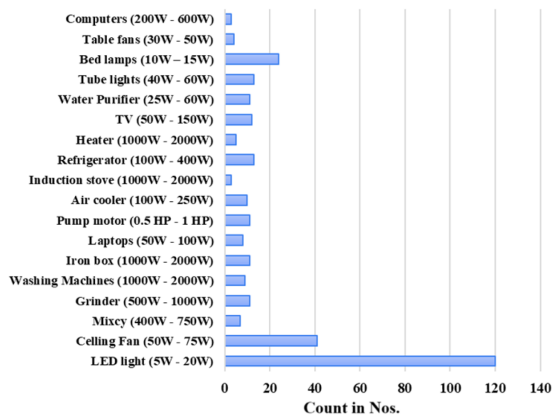
| Night time power demand | | | | |
|-------------------------|-----------|-------------|----------------------|--------------|
| House | Power (W) | Current (A) | Operating hours (Hr) | Amp. hr (Ah) |
| 1 | 3704 | 16.1 | 8 | 128.83 |
| 2 | 19,626 | 85.33 | 10 | 853.3 |
| 3 | 6761 | 29.4 | 6 | 176.37 |
| 4 | 7644 | 33.23 | 7 | 232.64 |
| 5 | 9603 | 41.75 | 7 | 292.27 |
| 6 | 5304 | 23.06 | 6 | 138.37 |
| 7 | 4289 | 18.65 | 6 | 111.89 |
| 8 | 2806 | 12.2 | 10 | 122 |
| 9 | 13,255 | 57.63 | 9 | 518.67 |
| 10 | 16,182 | 70.36 | 7 | 492.5 |
| Total | 89,174 | 388 | 76 | 3067 |

TABLE 3 | Total power calculated.

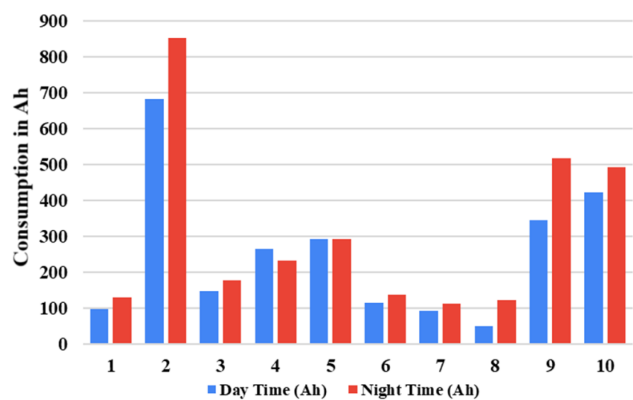
| Team | Total houses | Total power (kW) | Team | Total houses | Total power (kW) |
|------|--------------|------------------|-------|--------------|------------------|
| 1 | 10 | 77.74 | 24 | 10 | 35.16 |
| 2 | 10 | 145.71 | 25 | 10 | 56.70 |
| 3 | 5 | 34.90 | 26 | 10 | 59.70 |
| 4 | 10 | 40.94 | 27 | 10 | 89.25 |
| 5 | 6 | 24.50 | 28 | 10 | 89.17 |
| 6 | 10 | 40.26 | 29 | 10 | 56.70 |
| 7 | 5 | 24.86 | 30 | 10 | 50.00 |
| 8 | 10 | 36.19 | 31 | 10 | 30.00 |
| 9 | 10 | 40.46 | 32 | 10 | 56.70 |
| 10 | 10 | 39.02 | 33 | 10 | 39.02 |
| 11 | 5 | 131.44 | 34 | 7 | 8.00 |
| 12 | 7 | 33.00 | 35 | 10 | 25.00 |
| 13 | 10 | 54.80 | 36 | 10 | 56.70 |
| 14 | 10 | 66.99 | 37 | 10 | 56.70 |
| 15 | 10 | 108.53 | 38 | 5 | 34.90 |
| 16 | 10 | 35.60 | 39 | 10 | 39.02 |
| 17 | 10 | 40.00 | 40 | 10 | 60.22 |
| 18 | 10 | 35.34 | 41 | 10 | 33.99 |
| 19 | 10 | 41.69 | 42 | 10 | 83.12 |
| 20 | 10 | 35.81 | 43 | 10 | 11.00 |
| 21 | 10 | 54.25 | 44 | 10 | 29.98 |
| 22 | 10 | 102.78 | 45 | 10 | 21.20 |
| 23 | 10 | 56.70 | Total | 420 | 2323.74 |

4.1 | Wind Turbine System

The wind turbine is used for the conversion of wind kinetic energy to mechanical work. On the basis of relationships for the



(a)



(b)

FIGURE 1 | Power consumption (a) sample survey details (b) Ampere-hour in day time and night time.

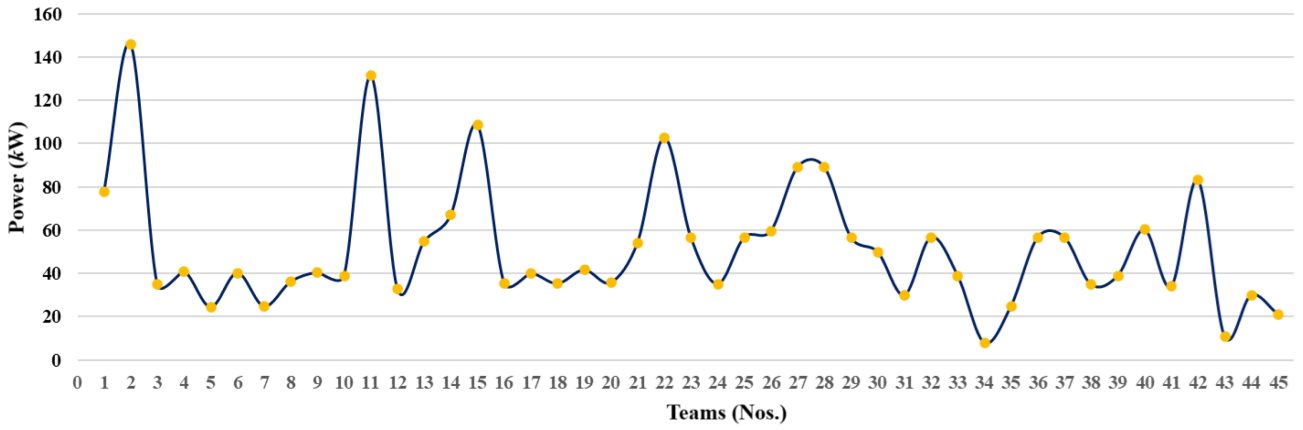


FIGURE 2 | Power consumption surveyed from 420 houses.

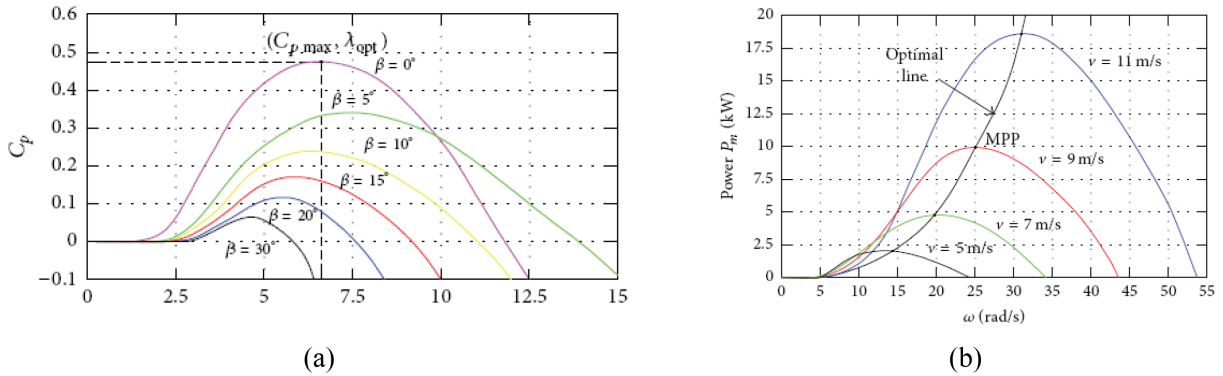


FIGURE 3 | Wind turbine characteristics (a) curve of power wind turbine coefficient (b) relationship between power and wind speed.

calculation, it is possible to express the value P_m of the aerodynamic wind turbine power.

$$P_m = 0.5\rho Av^3 C_p(\lambda, \beta) \quad (1)$$

The power coefficient $C_p(\gamma, \beta)$ can be computed as follows:

$$C_p(\lambda, \beta) = 0.22\left(\frac{116}{\lambda} - 0.4\beta - 5\right) \exp\left(-\frac{12.5}{\lambda}\right) \quad (2)$$

Here,

$$\frac{1}{\lambda} = \frac{1}{\lambda + 0.089} - \frac{0.035}{\beta^3 + 1} \quad (3)$$

The relationship between the wind speed and the rotor speed is defined as tip speed ratio γ :

$$\lambda = \frac{R\omega}{v} \quad (4)$$

The Figure 3 shows the Wind turbine characteristics. From the value of the rotational motion performance, it is possible to determine the value of the torque T_m acting on the shaft as follow:

$$T_m = \frac{P_m}{\omega} \quad (5)$$

The equations for the d -axis and q -axis currents are as,

$$\begin{cases} \frac{di_{sd}}{dt} = -\frac{R_{sd}}{L_{sd}} i_{sd} + \omega_s \frac{L_{sq}}{L_{sd}} i_{sq} + \frac{1}{L_{sd}} u_{sd} \\ \frac{di_{sq}}{dt} = -\frac{R_{sq}}{L_{sq}} i_{sq} - \omega_s \left(\frac{L_{sd}}{L_{sq}} i_{sd} + \frac{1}{L_{sq}} \Psi_p \right) + \frac{1}{L_{sq}} u_{sq} \end{cases} \quad (6)$$

The equation of the electromagnetic torque in the rotor is,

$$T_e = 1.5 \frac{P}{2} [\Psi_p i_{sq} + i_{sd} i_{sq} (L_{sd} - L_{sq})] \quad (7)$$

Figure 4 shows the dq -coordinates frame of the PMSG with θ being the angle between d -axis and the main stator axis.

4.2 | Modeling of the Solar PV System

The equivalent circuit of a PV cell is shown in Figure 5. The current source I_{ph} represents the cell photocurrent. R_{sh} and R_s are the intrinsic shunt and series resistances of the cell, respectively. Usually, the value of R_{sh} is very large and that of R_s is very small, hence they may be neglected to simplify the analysis. Practically, PV cells are grouped in larger units called PV modules and these modules are connected in series or parallel to create PV arrays which are used to generate electricity in PV generation systems. The voltage-current characteristic equation of a solar cell is provided as Module photo-current I_{ph} :

$$I_{ph} = [I_{sc} + K_1(T - 298)] \times \frac{I_r}{1000} \quad (8)$$

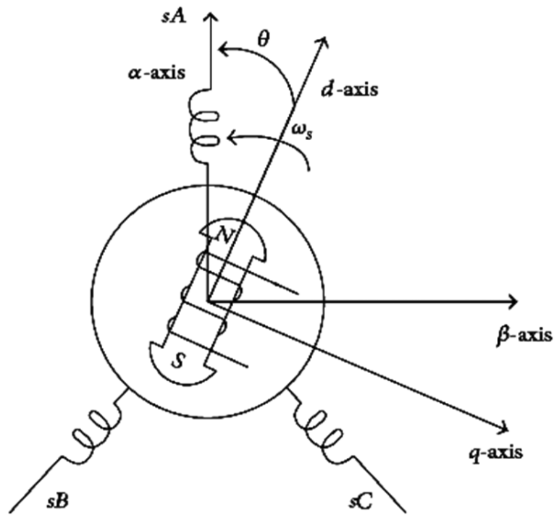


FIGURE 4 | dq-coordinates frame of the PMSG.

$$I_{rs} = \left[I_{sc} / \left[\exp\left(\frac{qV_{oc}}{N_s k n T} \right) - 1 \right] \right] \quad (9)$$

The module saturation current I_0 varies with the cell temperature, which is given by:

$$I_0 = I_{rs} \left[\frac{T}{T_r} \right]^3 \exp \left[\frac{qE_{g0}}{nk} \left(\frac{1}{T} - \frac{1}{T_r} \right) \right] \quad (10)$$

$$I = N_p \times I_{ph} - N_p \times I_0 \times \left[\exp \left(\frac{V}{N_s} + I \times \frac{R_s}{N_p} \right) - 1 \right] - I_{sh} \quad (11)$$

where $V_t = \frac{k \times T}{q}$.

4.3 | Modeling of the Hybrid Structure

PV-wind hybrid energy system's main components are shown in Figure 6. PV array and wind turbine generate energy for the

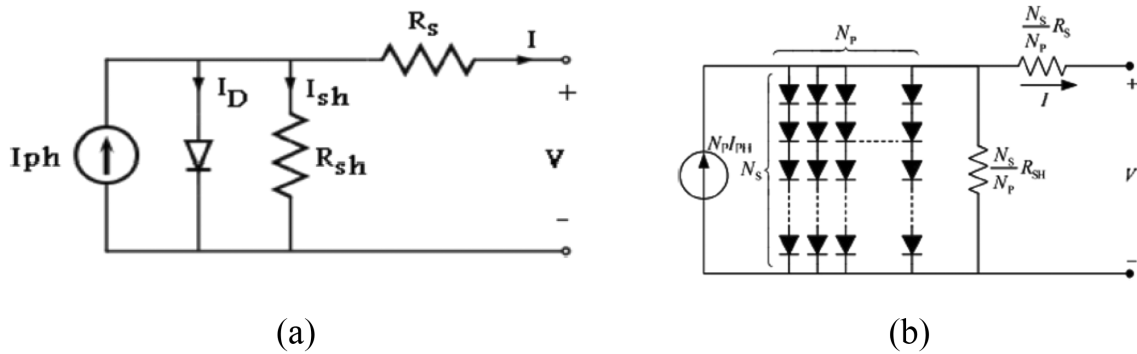


FIGURE 5 | Solar PV equivalent circuit (a) solar cell (b) solar array.

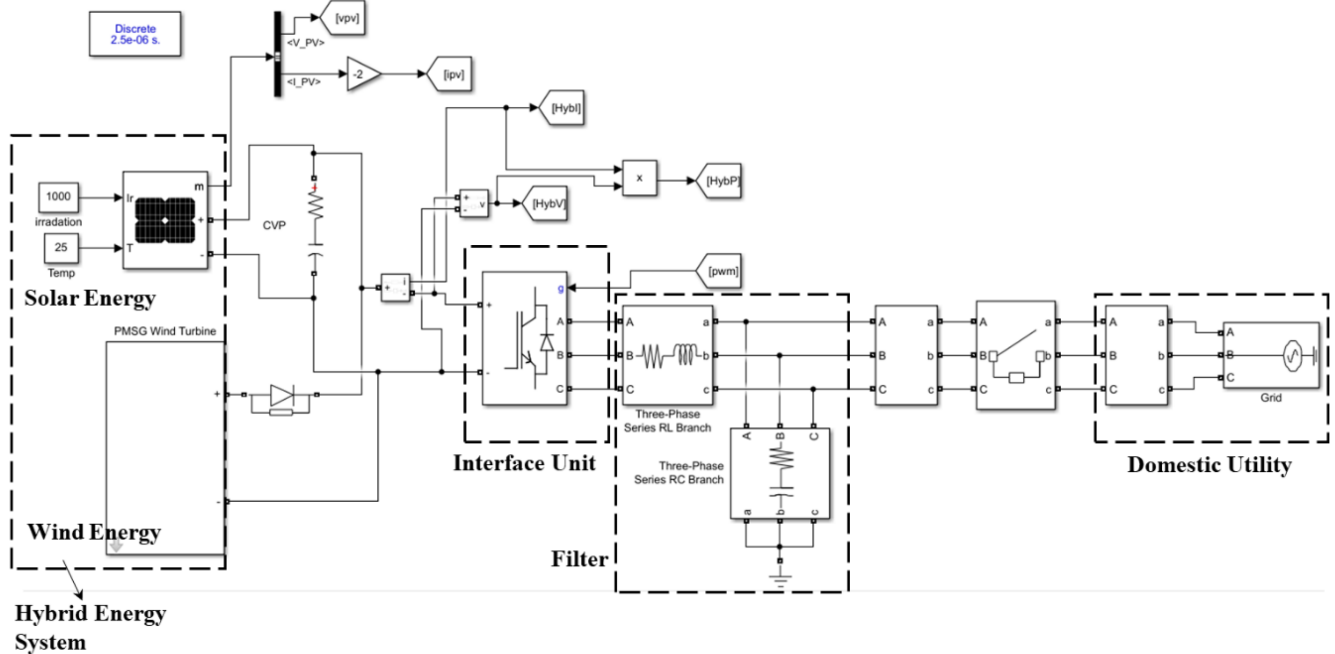


FIGURE 6 | Simulation model of proposed system.

load. Battery stores excess energy and supplies the load when the generated energy is not enough for the load. Battery charge controllers keep battery voltage within specific voltage window and thus, they prevent over discharge or overcharge regimes. To protect the battery against overcharging, PV array and wind generator is disconnected from the system when the DC bus voltage increases above $V_{\max\text{-off}}$ and when the current required by the load is less than the current generated by the PV array and wind generator. They are connected again when DC bus voltage decreases below $V_{\max\text{-on}}$. To protect the battery against excessive discharging, the load is disconnected when the DC bus voltage falls below $V_{\min\text{-off}}$ and when the current required by the load is greater than the current generated by the PV array and wind generator. The load is switched on when DC bus voltage increases above $V_{\min\text{-on}}$. The inverter converts generated energy from DC to AC for an AC load.

Batteries in a hybrid system are connected in series to obtain the appropriate nominal bus voltage. Therefore, the number of batteries connected in series for the same type of battery in a battery bank is calculated as follows,

$$N_{\text{SBat}} = \frac{V_{\text{pv}}}{V_{\text{Bat}}} \quad (12)$$

The hybrid system can have several different types of battery banks. The battery state of charge of a battery bank at time t is calculated based on adding the charge current (positive sign) or discharge current (negative sign) to the battery bank state of charge at the previous time instant. When adding the battery current to the battery state of charge, self-discharge losses and battery charging losses should be taken into account.

In a hybrid renewable energy system that uses batteries for energy storage and output regulation from intermittent sources like solar and wind, harmonics can be generated due to various reasons.

- In hybrid systems, the power electronic inverters are used to convert the DC power from the battery into AC power for the load or grid. These inverters generate harmonics due to the switching action of semiconductor devices.
- Many loads connected to the system, such as computers, LED lights, and variable frequency drives, are nonlinear in nature. These loads draw current in a non-sinusoidal manner, which introduces harmonic currents into the system. The harmonics generated by these loads can reflect back into the hybrid system, affecting the battery and other components.
- The process of charging and discharging the battery through converters or inverters can introduce harmonics. DC-DC converters and DC-AC inverters used for managing the energy flow to and from the battery can generate harmonic distortion in the power output.
- The variability in solar irradiance and wind speed can lead to fluctuations in the power generated by solar panels and wind turbines. This fluctuation may require rapid adjustments in the power electronics, resulting in the generation of harmonics.

The impact of harmonics in hybrid renewable energy systems can be minimized by designing a proper filter circuit, ensuring better power quality and system performance.

4.4 | Modeling of the LC-Filter

The proposed Solar-Wind Hybrid integration system is aimed at enhancing the power quality by connecting a filter circuit. A filter that can attenuate the harmonics generated by the power electronic components and ensure a smooth output is by designing the L-C component. An L-C filter is commonly used in renewable energy systems to reduce the harmonic distortion and smooth the AC output voltage and current. In a Solar-Wind Hybrid Renewable Energy System, the power generated by photovoltaic (PV) and wind turbine sources passes through inverters and other power electronics that produce high-frequency harmonics. These harmonics, if not filtered, can lead to power quality issues such as voltage distortion, reduced efficiency, and potential damage to connected loads. The L-C filter design involves determining suitable values for the inductance L_f and capacitance C_f , based on the desired cutoff frequency f_c and impedance requirements. The cutoff frequency f_c can be given as in (13),

$$f_c = \frac{1}{2\pi\sqrt{LC}} \quad (13)$$

The filter inductor L_f and filter capacitor C_f values are chosen to provide enough impedance at higher frequencies, thereby blocking or reducing harmonic currents. It is calculated as in (14),

$$\begin{cases} L_f = \frac{V_{\text{dc}}}{4\pi f_s I_{\text{ac}}} \\ C_f = \frac{1}{(2\pi f_c)^2 L} \end{cases} \quad (14)$$

where, V_{dc} is the dc-link voltage, f_s is the converter switching frequency, f_c is the cut-off frequency and I_{ac} is the ac output current.

The filter is designed to achieve a specified reduction in THD, ensuring that the harmonic content falls within acceptable limits (e.g., THD < 5%). For the dc-link voltage of 1000 V, the ac current I_{ac} of 2.5 kA, switching frequency f_s of 1 kHz, the filter inductor L_f is 3.2 mH and inductor C_f is 1.6 μF .

5 | Results and Discussion

The proposed system is a hybrid power distribution setup combining solar and wind energy sources to enhance the reliability and sustainability of electricity supply. This hybrid system integrates both solar photovoltaic (PV) panels and wind turbines to generate renewable energy, which is then distributed to the utility grid serving 420 homes within the community. In this hybrid system, the solar energy is harnessed through photovoltaic panels, which convert sunlight directly into electricity. Simultaneously, wind turbines capture the kinetic energy of the wind and convert it into mechanical power, which is then transformed into electrical energy. By leveraging both solar and wind resources, the system aims to provide a more consistent and reliable power supply, overcoming the limitations of each individual energy source. The

TABLE 4 | Simulation design parameters of the proposed system.

| Parameter | Value |
|------------------------------------|-----------------------------------|
| Solar PV system | |
| Rated power output | 1.5 MW |
| Number of solar panels | 2500 |
| Type of solar panel | Monocrystalline |
| Rated voltage of each panel | 36 V |
| Rated current of each panel | 8 A |
| Total array voltage | 750 V |
| Total array current | 20 kA |
| Efficiency of PV modules | 20% |
| Tilt angle of panels | (15–35) deg. |
| Maximum power point tracker (MPPT) | P & O |
| Temperature coefficient | 0.4%/°C |
| Wind energy system | |
| Rated power output | 0.5 MW (500 kW) |
| Type of wind turbine | HAWT |
| Rotor diameter | 45 m |
| Hub height | 60 m |
| Cut-in wind speed | 3 m/s |
| Rated wind speed | 12 m/s |
| Cut-out wind speed | 25 m/s |
| Number of blades | 3 |
| Generator type | Synchronous Generator |
| Tip-speed ratio (λ) | 7.5 |
| Efficiency of wind turbine | 40% |
| Control system | Pitch Control |
| Brake system | Mechanical and Aerodynamic Brakes |
| Battery capacity | |
| Rated capacity | 500 kWh |
| Battery type | Lithium-ion (Li-ion) |
| Nominal voltage | 400 V |
| Nominal current | 1250 A |
| Depth of discharge (DoD) | 80% |
| Charge/discharge efficiency | 95% |
| Battery lifetime | 5000 cycles |
| Charging time | 4 h |
| Discharge time | 2 h |
| Operating temperature range | 0 to 40°C |
| Battery pack configuration | 400 V system |
| Energy density | 200 Wh/kg |
| Cycle life | 5000 cycles (at 80% DoD) |
| Self-discharge rate | 2%–3% per month |

(Continues)

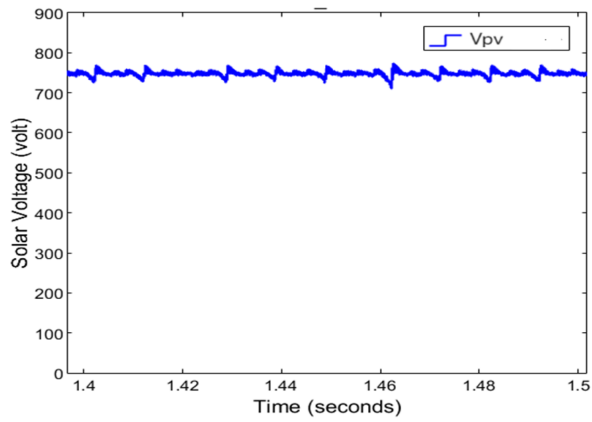
TABLE 4 | (Continued)

| Parameter | Value |
|------------------------------|-------------------------------------|
| Grid interface system | |
| Total connected load | 2.3 MW |
| Type of load | Mixed residential and commercial |
| Peak load demand | 2.3 MW |
| Average load demand | 1.8 MW |
| Load power factor | 0.9 (lagging) |
| Grid voltage level | 400 V (3-phase, 50 Hz) |
| Grid connection type | 3-phase, 4-wire |
| Load current | 3320 A (for peak load) |
| Load diversity factor | 0.8 |
| Critical loads | 500 kW |
| Non-critical loads | 1.8 MW |
| Frequency regulation | ± 0.1 Hz |
| Short circuit level | 25 kA (at point of common coupling) |

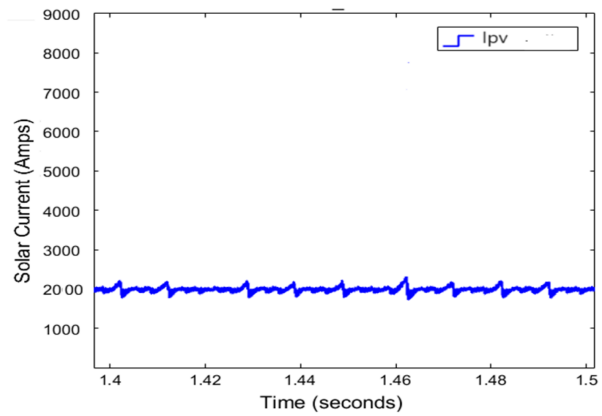
generated power is fed into the utility grid, ensuring that the electricity needs of the 420 homes are met efficiently. This setup not only reduces dependence on traditional non-renewable energy sources but also enhances the grid's resilience to fluctuations in energy demand and supply. The proposed system is mathematically modeled in MATLAB/Simulink. The design parameters are shown in the Table 4.

Figure 6 illustrates a comprehensive simulation diagram of the proposed hybrid power distribution system. This diagram provides a visual representation of the various components involved, including the solar PV panels, wind turbines, energy storage units, and the connection to the utility grid. It highlights the integration of these components and the flow of electricity from generation to distribution. The simulation diagram helps in understanding the overall architecture of the system, the interactions between different components, and the pathways through which energy is managed and supplied. By combining solar and wind energy, the system aims to optimize power generation and distribution, ensuring a stable and sustainable energy supply for the community.

The proposed system integrates a hybrid solar-wind configuration to power the entire setup efficiently. This hybrid approach leverages both solar photovoltaic (PV) panels and wind turbines to ensure a reliable and continuous energy supply. Figure 7 illustrates the voltage and current characteristics of the solar PV system component. According to the figure, the solar PV system generates a voltage of 750 volts (V) and a current of 20 amps (A). These parameters are crucial for understanding the performance and efficiency of the solar PV system in the hybrid setup. The voltage of 750 V indicates the electrical potential generated by the solar panels, which is a result of the panels' configuration and the intensity of sunlight they receive. The current of 20 A reflects the amount of electrical current produced, which, together with the voltage, determines the power output of the solar PV system.

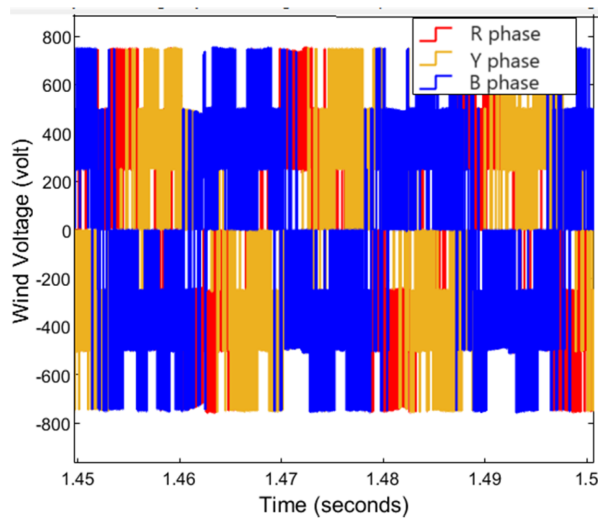


(a)

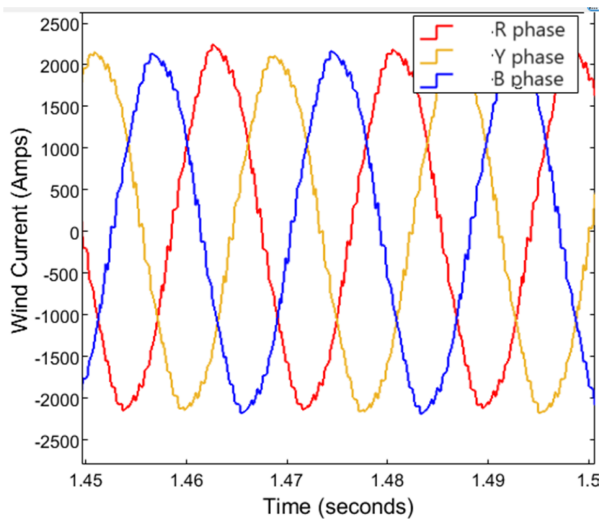


(b)

FIGURE 7 | Solar PV (a) voltage (b) current.



(a)



(b)

FIGURE 8 | Wind energy conversion system (a) voltage (b) current.

The wind power generated by the Permanent Magnet Synchronous Generator (PMSG) wind turbine is illustrated in Figure 8. This figure provides critical data on the performance of the Wind Energy Conversion System (WECS). Specifically, it shows that the WECS produces a voltage of 600 volts (V) and a current of 2000 amps (A). The voltage of 600 V represents the electrical potential generated by the PMSG wind turbine, which is crucial for effective energy conversion and integration into the hybrid system. The high current of 2000 A indicates the significant amount of electrical current produced by the turbine, which, along with the voltage, determines the total power output of the wind energy system.

The simulation results of the proposed hybrid solar-wind power system, conducted using MATLAB, provide valuable insights into its performance at various points within the system. Figure 9 illustrates the voltage and current waveforms obtained at the input side of the system. The three-phase (3 Φ) voltage is measured at 400 volts (V), and the current is recorded at

1000 amps (A). These parameters are crucial for understanding the system's electrical characteristics. The voltage of 400 V represents the electrical potential present at the input side, which is vital for efficient power transfer and integration with the utility grid. The high current of 1000 A indicates the significant flow of electrical current through the system. Together with the voltage, this current value helps determine the overall power output and efficiency of the hybrid system. These simulated waveforms are essential for evaluating the performance and stability of the hybrid power system. They provide a detailed view of how the system handles and distributes energy, ensuring that it can meet the requirements for effective integration into the utility grid. The results from MATLAB simulations confirm the capability of the hybrid system to manage and deliver power reliably, supporting its application for community energy needs.

The voltage and current Total Harmonic Distortions (THDs) were measured using Fast Fourier Transform (FFT) analysis over a time duration from 0.1 to 0.2 s. Figure 10a presents the THD of

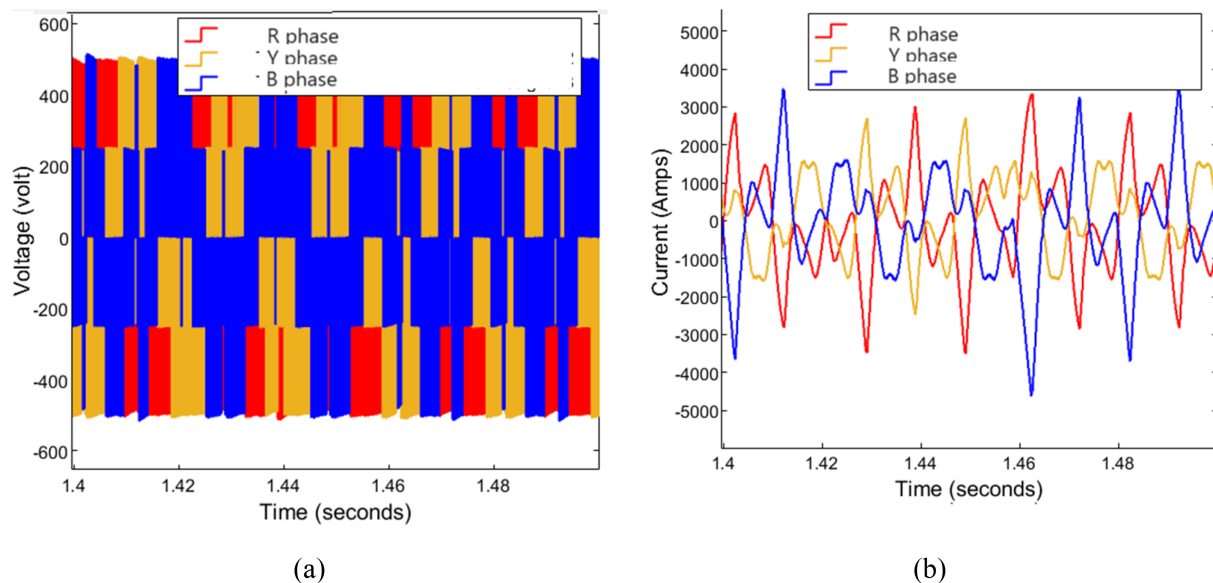


FIGURE 9 | Input side grid (a) voltage (b) current.

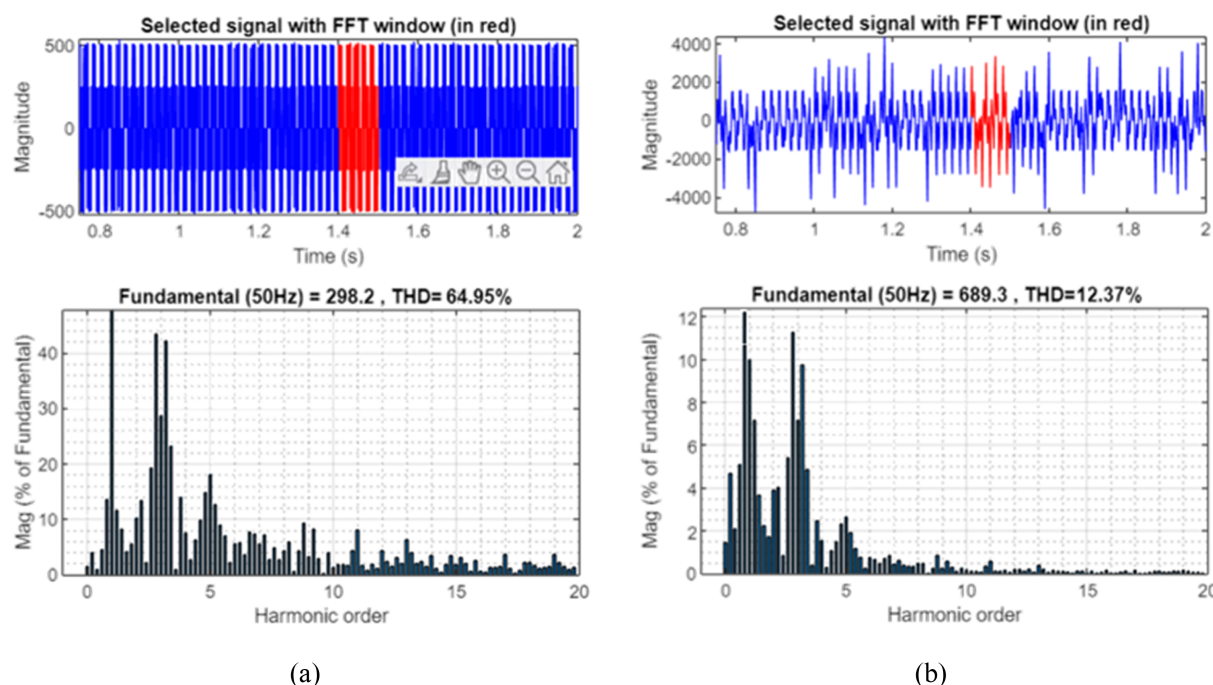


FIGURE 10 | Input side grid THDs (a) voltage (b) current.

the voltage, which was found to be 64.95%. This high level of voltage THD indicates significant harmonic distortion in the voltage waveform, which can impact the overall power quality and efficiency of the system. In contrast, Figure 10b shows the THD for the current, which is recorded at 12.37%. Although this value is lower than the voltage THD, it still reflects some level of harmonic distortion present in the current waveform. The difference between the voltage and current THDs highlights the varying degrees of distortion in different parts of the system. Analyzing these THD values is crucial for assessing the performance and quality of the power generated by the hybrid system. High THD in

the voltage can lead to issues such as increased losses, overheating, and reduced system efficiency, while high current THD can affect the reliability and stability of the power supply. The FFT analysis provides detailed insights into these distortions, helping to identify potential areas for improvement and optimization in the system design and operation.

The utility grid, which serves the load of 420 houses in the community, necessitates a low Total Harmonic Distortion (THD) to ensure high power quality and efficiency. To achieve this, filtering components are employed to minimize harmonic distortions in the output power. Figure 11 displays the characteristics

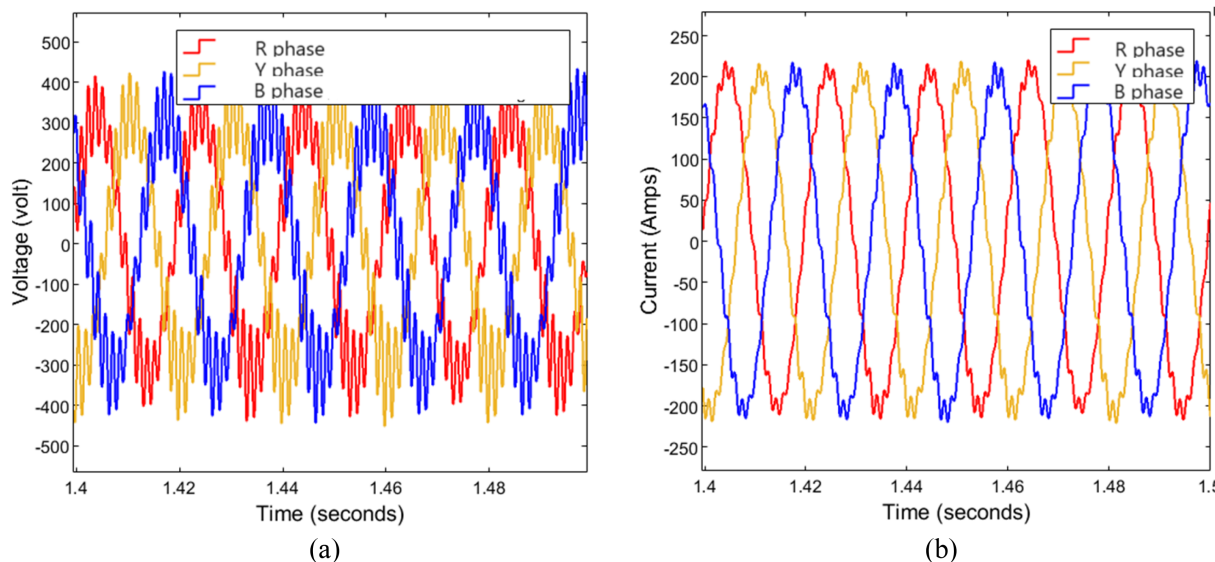


FIGURE 11 | Utility side with filter (a) voltage (b) current.

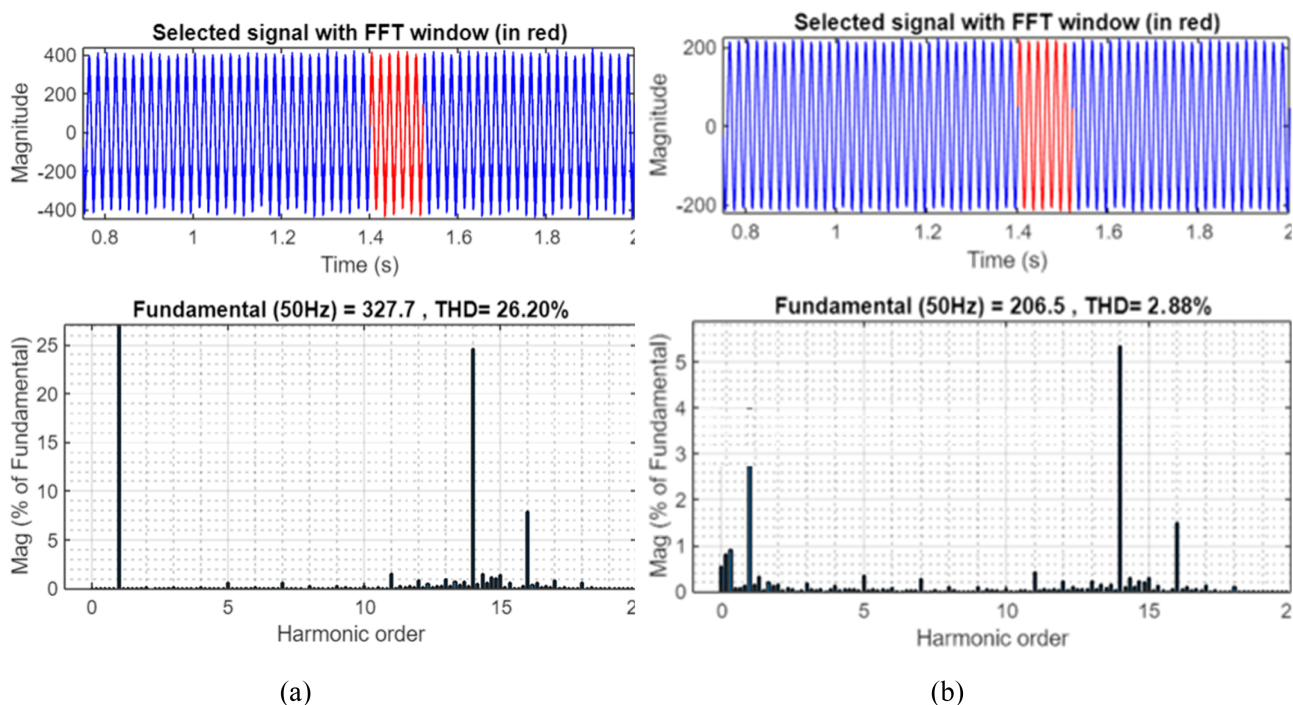


FIGURE 12 | Utility side grid THDs (a) voltage (b) current.

of the voltage and current at the utility grid side after incorporating these filters. The voltage at the utility grid side is measured at 400 volts (V), which is consistent with the required standard for stable grid integration. Additionally, the current delivered to the grid is 200 amps (A). The use of filtering components effectively reduces the harmonic distortions, thereby improving the overall quality of the power supplied to the community. This approach ensures that the power delivered meets the stringent requirements for low THD, enhancing both the reliability and efficiency of the hybrid power system. The implementation of these filters is crucial for maintaining the integrity of the power supply and ensuring that it adheres to regulatory standards for

grid-connected systems. By addressing the harmonic distortions, the filtering components contribute to a more stable and efficient energy distribution, benefiting the overall performance of the hybrid solar-wind system.

The effectiveness of the filtering components at the utility grid side is evident from the Total Harmonic Distortion (THD) values obtained through FFT analysis, as shown in Figure 12. Following the application of these filters, the voltage THD has decreased to 26.20%, while the current THD has been reduced to 2.88%. These improvements signify a significant reduction in harmonic distortions, enhancing the quality of the power supplied to the

utility grid. The reduction in voltage THD from previous levels indicates that the filters are effectively minimizing the harmonic content in the voltage waveform, which is crucial for maintaining stable and reliable power quality. Similarly, the decrease in current THD demonstrates a marked improvement in the harmonic content of the current, further contributing to a more efficient and stable energy supply. The lower THD values highlight the success of the filtering approach in addressing harmonic issues, thus ensuring that the power delivered to the community adheres to the necessary standards for grid integration. This reduction in distortions not only improves the overall performance of the hybrid solar-wind system but also enhances the reliability and efficiency of the power distribution to the 420 houses served by the utility grid.

The Total Harmonic Distortion (THD) of voltage and current is a crucial factor in assessing the power quality of a grid system. Figure 8 illustrates the input side grid voltage and current over

time in a three-phase system. The Fast Fourier Transform (FFT) analysis performed between 0.1 and 0.2 s reveals significant THD levels: 64.95% for voltage and 12.37% for current. This analysis was conducted without the use of filtering components, at a frequency of 50 Hz. In contrast, Figure 10 shows the utility side voltage and current over the same time period and in the same three-phase configuration. With the implementation of filters, the FFT analysis results indicate a substantial reduction in THD, with values dropping to 26.20% for voltage and 2.88% for current. This analysis was also performed at a frequency of 50 Hz but with the filtering components in place.

The comparison of THD values, both with and without filtering, is summarized in Figure 13. This comparison highlights the effectiveness of the filtering approach in mitigating harmonic distortions. The reduction in voltage THD from 64.95% to 26.20% and in current THD from 12.37% to 2.88% demonstrates a marked improvement in power quality. These

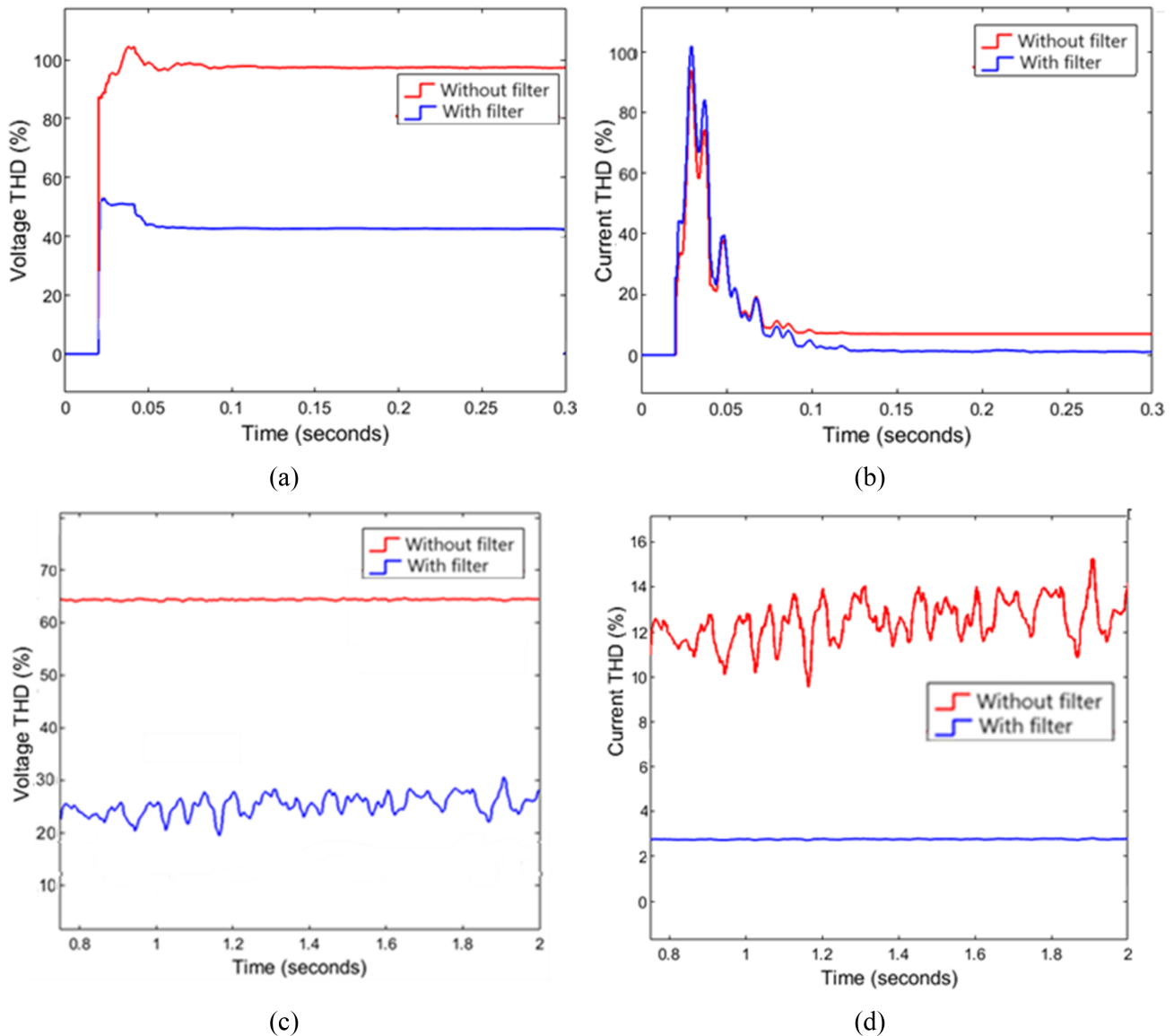


FIGURE 13 | THD comparison with and without filters (a) existing system voltage (b) existing system current (c) proposed system voltage (d) proposed system current.

TABLE 5 | THD comparison of existing and proposed system.

| THDs | Existing system | | Proposed system | |
|---------|-----------------|-------------|-----------------|-------------|
| | Without filter | With filter | Without filter | With filter |
| Voltage | 97.85% | 45.48% | 64.95% | 26.20% |
| Current | 16.52% | 8.32% | 12.37% | 2.88% |

results emphasize the critical role of filtering components in enhancing the performance and reliability of the hybrid solar-wind power system by significantly reducing harmonic distortions.

Based on the analysis of the figures, the THD values obtained for both the input and utility grid sides are summarized and tabulated in Table 5. This table provides a comprehensive comparison of the Total Harmonic Distortion (THD) for voltage and current before and after the implementation of filtering components.

It can be inferred that the Total Harmonic Distortion (THD) values observed in existing systems using non-renewable energy sources typically fall within acceptable limits and meet standard requirements. However, the primary focus is on transitioning from non-renewable to renewable energy sources to enhance sustainability and reduce environmental impact. To address this, the proposed hybrid solar-wind system was simulated to power similar utilities, aiming to achieve comparable THD levels. The simulation results for the proposed renewable energy system indicate that the THD values obtained are similar to those of the existing non-renewable system. This suggests that the proposed system effectively maintains power quality standards while utilizing renewable resources.

In this study, a hybrid solar-wind power system was designed and simulated to address power quality issues in a domestic grid application. The results demonstrate that the hybrid system, which combines solar and wind energy, effectively maintains high power quality standards. Initially, the Total Harmonic Distortion (THD) values were significantly high, with 64.95% for voltage and 12.37% for current at the input side without filters. However, after the integration of filtering components, these values improved substantially to 26.20% for voltage and 2.88% for current at the utility grid side. The THD levels achieved by the proposed system are comparable to those of existing non-renewable energy systems, as depicted in Figure 12, which highlights the system's ability to deliver similar power quality. This indicates that the hybrid solar-wind system not only meets the required standards for power quality but also demonstrates the potential to effectively replace non-renewable sources with renewable ones without compromising performance. The study underscores the feasibility of integrating hybrid renewable energy systems into existing grids, offering a sustainable alternative that aligns with environmental goals while maintaining grid reliability and efficiency. The successful implementation of filtering components further ensures that the system minimizes harmonic distortions, contributing to a stable and high-quality power supply.

6 | Conclusion

In conclusion, this study successfully demonstrates the viability and effectiveness of a hybrid solar-wind power system for domestic grid applications. The simulation results reveal that the proposed system maintains high power quality standards by effectively managing Total Harmonic Distortion (THD) levels. Initially, without filtering, the THD values were notably high—64.95% for voltage and 12.37% for current. However, the incorporation of filtering components resulted in substantial improvements, reducing THD to 26.20% for voltage and 2.88% for current. These results confirm that the hybrid solar-wind system can deliver power quality comparable to existing non-renewable energy systems. This suggests that the transition to renewable energy sources, while maintaining performance standards, is not only feasible but also beneficial for sustainable power generation. Furthermore, this study highlights the practical implications of hybrid renewable energy systems, such as reduced greenhouse gas emissions by displacing fossil fuel use and contributing to the decarbonization of the energy sector. It also emphasizes economic benefits, particularly through cost savings on electricity bills for households and businesses, as well as long-term investment potential in renewable energy infrastructure. The scalability of the system allows it to be adapted for a variety of applications, from residential to commercial, further underscoring its flexibility and relevance in diverse geographical and economic contexts.

Author Contributions

F. Max Savio: conceptualization, investigation, methodology, formal analysis. **S. Vinson Joshua:** investigation, writing – original draft, validation. **K. Usha:** conceptualization, software, project administration, writing – review and editing, methodology. **Muhammad Faheem:** methodology, validation, visualization, writing – review and editing, project administration, supervision. **Raju Kannadasan:** resources, data curation, project administration, validation, investigation, conceptualization. **Arfat Ahmad Khan:** conceptualization, methodology, validation, writing – review and editing, resources.

Conflicts of Interest

The authors declare no conflicts of interest.

Data Availability Statement

Data sharing not applicable to this article as no datasets were generated or analysed during the current study.

References

1. W. A. Eltayeb, J. Somlal, S. Kumar, and S. K. Rao, "Design and Analysis of a Solar-Wind Hybrid Renewable Energy Tree," *Results in Engineering* 17 (2023): 100958, <https://doi.org/10.1016/j.rineng.2023.100958>.
2. Q. Hassan, S. Algburi, A. Z. Sameen, H. M. Salman, and M. Jaszczur, "A Review of Hybrid Renewable Energy Systems: Solar and Wind-Powered Solutions: Challenges, Opportunities, and Policy Implications," *Results in Engineering* 20 (2023): 101621, <https://doi.org/10.1016/j.rineng.2023.101621>.
3. S. Ravikumar, H. Vennila, and R. Deepak, "Hybrid Power Generation System With Total Harmonic Distortion Minimization Using Improved Rider Optimization Algorithm: Analysis on Converters," *Journal of*

- Power Sources* 459 (2020): 228025, <https://doi.org/10.1016/j.jpowsour.2020.228025>.
4. P. A. Gbadega and O. A. Balogun, "Modeling and Control of Grid-Connected Solar-Wind Hybrid Micro-Grid System With Multiple-Input Ćuk DC-DC Converter for Household & High Power Applications," *International Journal of Engineering Research in Africa* 58 (2022): 191–224, <https://doi.org/10.4028/www.scientific.net/jera.58.191>.
5. S. Jahan, S. P. Biswas, M. K. Hosain, et al., "An Advanced Control Technique for Power Quality Improvement of Grid-Tied Multilevel Inverter," *Sustainability* 13 (2021): 505, <https://doi.org/10.3390/su13020505>.
6. F. Al-Turjman, Z. Qadir, M. Abujubbeh, and C. Batunlu, "Feasibility Analysis of Solar Photovoltaic-Wind Hybrid Energy System for Household Applications," *Computers and Electrical Engineering* 86 (2020): 106743, <https://doi.org/10.1016/j.compeleceng.2020.106743>.
7. P. Roy, J. He, T. Zhao, and Y. V. Singh, "Recent Advances of Wind-Solar Hybrid Renewable Energy Systems for Power Generation: A Review," *IEEE Open Journal of the Industrial Electronics Society* 3 (2022): 81–104, <https://doi.org/10.1109/OJIES.2022.3144093>.
8. Y. Chen, M. Quan, D. Wang, et al., "Energy, Exergy, and Economic Analysis of a Solar Photovoltaic and Photothermal Hybrid Energy Supply System for Residential Buildings," *Building and Environment* 243 (2023): 110654, <https://doi.org/10.1016/j.buildenv.2023.110654>.
9. A. K. Hamid, N. T. Mbungu, A. Elnady, R. C. Bansal, A. A. Ismail, and M. A. AlShabi, "A Systematic Review of Grid-Connected Photovoltaic and Photovoltaic/Thermal Systems: Benefits, Challenges and Mitigation," *Energy & Environment* 34, no. 7 (2023): 2775–2814, <https://doi.org/10.1177/0958305X221117617>.
10. M. N. Ayesha, M. F. Baig, and M. Yousif, "Reliability Evaluation of Energy Storage Systems Combined With Other Grid Flexibility Options: A Review," *Journal of Energy Storage* 63 (2023): 107022, <https://doi.org/10.1016/j.est.2023.107022>.
11. S. Algarni, V. Tirth, T. Alqahtani, S. Alshehery, and P. Kshirsagar, "Contribution of Renewable Energy Sources to the Environmental Impacts and Economic Benefits for Sustainable Development," *Sustainable Energy Technologies and Assessments* 56 (2023): 103098, <https://doi.org/10.1016/j.seta.2023.103098>.
12. J. Li, J. Shao, X. Yao, and J. Li, "Life Cycle Analysis of the Economic Costs and Environmental Benefits of Photovoltaic Module Waste Recycling in China," *Resources, Conservation and Recycling* 196 (2023): 107027, <https://doi.org/10.1016/j.resconrec.2023.107027>.
13. M. Kamal, A. Bostani, J. L. Webber, A. Mehbodniya, R. Mishra, and M. Arumugam, "Total Harmonic Distortion Reduction Based Energy Harvesting Using Grid-Based Three Phase System and Integral-Derivative," *Computers and Electrical Engineering* 109 (2023): 108744, <https://doi.org/10.1016/j.compeleceng.2023.108744>.
14. S. Murugesan and M. V. Suganyadevi, "Performance Analysis of Simplified Seven-Level Inverter Using Hybrid HHO-PSO Algorithm for Renewable Energy Applications," *Iranian Journal of Science & Technology Transactions of Electrical Engineering* 48 (2024): 781–801, <https://doi.org/10.1007/s40998-023-00676-9>.
15. T. Wilberforce, A. G. Olabi, E. T. Sayed, A. H. Alalmi, and M. A. Abdelkareem, "Wind Turbine Concepts for Domestic Wind Power Generation at Low Wind Quality Sites," *Journal of Cleaner Production* 394 (2023): 136137, <https://doi.org/10.1016/j.jclepro.2023.136137>.
16. M. Khalid, "Smart Grids and Renewable Energy Systems: Perspectives and Grid Integration Challenges," *Energy Strategy Reviews* 51 (2024): 101299, <https://doi.org/10.1016/j.esr.2024.101299>.
17. A. N. Mulumba and H. Farzaneh, "Techno-Economic Analysis and Dynamic Power Simulation of a Hybrid Solar-Wind-Battery-Flywheel System for Off-Grid Power Supply in Remote Areas in Kenya," *Energy Conversion and Management: X* 18 (2023): 100381, <https://doi.org/10.1016/j.ecmx.2023.100381>.
18. O. K. Olajiga, E. C. Ani, T. M. Olatunde, and Z. Q. Sikhakane, "Assessing the Potential of Energy Storage Solutions for Grid Efficiency: A Review," *Engineering Science & Technology Journal* 5, no. 3 (2024): 1112–1124, <https://doi.org/10.51594/estj.v5i3.974>.
19. E. A. Etukudoh, A. Fabuyide, K. I. Ibekwe, S. Sonko, and V. I. Ilojiana, "Electrical Engineering in Renewable Energy Systems: A Review of Design and Integration Challenges," *Engineering Science & Technology Journal* 5, no. 1 (2024): 231–244, <https://doi.org/10.51594/estj.v5i1.746>.
20. B. Atilgan Turkmen and F. Germirli Babuna, "Life Cycle Environmental Impacts of Wind Turbines: A Path to Sustainability With Challenges," *Sustainability* 16 (2024): 5365, <https://doi.org/10.3390/su16135365>.
21. M. Thirunavukkarasu, Y. Sawle, and H. Lala, "A Comprehensive Review on Optimization of Hybrid Renewable Energy Systems Using Various Optimization Techniques," *Renewable and Sustainable Energy Reviews* 176 (2023): 113192, <https://doi.org/10.1016/j.rser.2023.113192>.
22. T. Pan, Z. Wang, J. Tao, and H. Zhang, "Operating Strategy for Grid-Connected Solar-Wind-Battery Hybrid Systems Using Improved Grey Wolf Optimization," *Electric Power Systems Research* 220 (2023): 109346, <https://doi.org/10.1016/j.epsr.2023.109346>.
23. M. U. Manoo, F. Shaikh, L. Kumar, and M. Arıcı, "Comparative Techno-Economic Analysis of Various Stand-Alone and Grid Connected (Solar/Wind/Fuel Cell) Renewable Energy Systems," *International Journal of Hydrogen Energy* 52 (2024): 397–414, <https://doi.org/10.1016/j.ijhydene.2023.05.258>.
24. A. Panda, A. K. Dauda, H. Chua, R. R. Tan, and K. B. Aviso, "Recent Advances in the Integration of Renewable Energy Sources and Storage Facilities with Hybrid Power Systems," *Cleaner Engineering and Technology* 12 (2023): 100598, <https://doi.org/10.1016/j.clet.2023.100598>.
25. S. K. H. Shah, A. Hellany, M. Nagrial, and J. Rizk, "Influence of Environmental Changes on Power Quality Disturbances in Hybrid Renewable Energy System," *Energy Reports* 9, no. Supplement 11 (2023): 164–173, <https://doi.org/10.1016/j.egy.2023.08.047>.
26. B. Modu, M. P. Abdullah, A. L. Bukar, and M. F. Hamza, "A Systematic Review of Hybrid Renewable Energy Systems With Hydrogen Storage: Sizing, Optimization, and Energy Management Strategy," *International Journal of Hydrogen Energy* 48, no. 97 (2023): 38354–38373, <https://doi.org/10.1016/j.ijhydene.2023.06.126>.
27. A. Owosuhi, Y. Hamam, and J. Munda, "Maximizing the Integration of a Battery Energy Storage System–Photovoltaic Distributed Generation for Power System Harmonic Reduction: An Overview," *Energies* 16 (2023): 2549, <https://doi.org/10.3390/en16062549>.
28. Z. Hu, Y. Han, A. S. Zalhaf, S. Zhou, E. Zhao, and P. Yang, "Harmonic Sources Modeling and Characterization in Modern Power Systems: A Comprehensive Overview," *Electric Power Systems Research* 218 (2023): 109234, <https://doi.org/10.1016/j.epsr.2023.109234>.
29. A. Mansouri, A. El Magri, R. Lajouad, I. El Myasse, E. K. Younes, and F. Giri, "Wind Energy Based Conversion Topologies and Maximum Power Point Tracking: A Comprehensive Review and Analysis," *e-Prime Advances in Electrical Engineering, Electronics and Energy* 6 (2023): 100351, <https://doi.org/10.1016/j.prime.2023.100351>.
30. Z. Reguieg, I. Bouyakoub, and F. Mehedi, "Optimizing Power Quality in Interconnected Renewable Energy Systems: Series Active Power Filter Integration for Harmonic Reduction and Enhanced Performance," *Electrical Engineering* 5 (2024), 10231, <https://doi.org/10.1007/s00202-024-02489-3>.
31. A. Argüello, R. Torquato, and W. Freitas, "Passive Filter Tuning for Harmonic Resonance Mitigation in Wind Parks," *IEEE Transactions on Power Delivery* 38, no. 6 (2023): 3834–3846, <https://doi.org/10.1109/TPWRD.2023.3291817>.
32. D. K. Dash and P. K. Sadhu, "A Review on the Use of Active Power Filter for Grid-Connected Renewable Energy Conversion Systems," *Processes* 11 (2023): 1467, <https://doi.org/10.3390/pr11051467>.

33. W. Guo and W. Xu, "Research on Optimization Strategy of Harmonic Suppression and Reactive Power Compensation of Photovoltaic Multi-functional Grid Connected Inverter," *International Journal of Electrical Power & Energy Systems* 145 (2023): 108649, <https://doi.org/10.1016/j.ijepes.2022.108649>.
34. T. E. Rao, E. Sundaram, S. Chenniappan, D. Almakhlles, U. Subramaniam, and M. S. Bhaskar, "Performance Improvement of Grid Interfaced Hybrid System Using Distributed Power Flow Controller Optimization Techniques," *IEEE Access* 10 (2022): 12742, <https://doi.org/10.1109/ACCESS.2022.3146412>.
35. A. A. A. Radwan and Y. A.-R. I. Mohamed, "Grid-Connected Wind-Solar Cogeneration Using Back-to-Back Voltage-Source Converters," *IEEE Transactions on Sustainable Energy* 11, no. 1 (2020): 315–325, <https://doi.org/10.1109/TSTE.2019.2890828>.
36. N. Kanagaraj, M. Vijayakumar, M. Ramasamy, and O. Aldosari, "Energy Management and Power Quality Improvement of Hybrid Renewable Energy Generation System Using Coordinated Control Scheme," *IEEE Access* 11 (2023): 93254, <https://doi.org/10.1109/ACCESS.2023.3299035>.
37. M. Faheem, M. A. Al-Khasawneh, A. A. Khan, and S. H. H. Madni, "Cyberattack Patterns in Blockchain-Based Communication Networks for Distributed Renewable Energy Systems: A Study on Big Datasets," *Data in Brief* 53, no. 5 (2024a): 110212, <https://doi.org/10.1016/j.dib.2024.11021250>.
38. B. Raza, Y. J. Kumar, A. K. Malik, A. Anjum, and M. Faheem, "Performance Prediction and Adaptation for Database Management System Workload Using Case-Based Reasoning Approach," *Information Systems* 76, no. 5 (2018): 46–58, <https://doi.org/10.1016/j.is.2018.04.00551>.
39. M. Faheem and A.-K. Mahmoud Ahmad, "Multilayer Cyberattacks Identification and Classification Using Machine Learning in Internet of Blockchain (IoBC)-Based Energy Networks," *Data in Brief* 54, no. 5 (2024): 110461, <https://doi.org/10.1016/j.dib.2024.110461>.
40. B. Raza, A. Aslam, A. Sher, A. K. Malik, and M. Faheem, "Autonomic Performance Prediction Framework for Data Warehouse Queries Using Lazy Learning Approach," *Applied Soft Computing* 91 (2020): 106216, <https://doi.org/10.1016/j.asoc.2020.10621648>.
41. M. Faheem, B. Raza, M. S. Bhutta, and S. H. H. Madni, "A Blockchain-Based Resilient and Secure Framework for Events Monitoring and Control in Distributed Renewable Energy Systems," *IET Blockchain* 1–15 (2024b), <https://doi.org/10.1049/blc2.12081>.
42. M. Faheem, M. Umar, R. A. Butt, B. Raza, M. A. Ngadi, and V. C. Gungor, "Software Defined Communication Framework for Smart Grid to Meet Energy Demands in Smart Cities," in *2019 7th International Istanbul Smart Grids and Cities Congress and Fair (ICSG)* (2019), 51–55.